Lasers in Surgery and Medicine 22:51–57 (1998)

Interstitial Laser-Induced Thermotherapy: Influence of Carbonization on Lesion Size

Christian Sturesson, MSc

Department of Physics, Lund Institute of Technology, S-22100 Lund, Sweden

Background and Objective: **The size of laser-induced coagulated lesions produced in porcine muscle in vitro using a cylindrical diffusing fiber tip and a conductive heat source, made by covering the diffuser with a hollow steel needle, were compared to investigate the influence of charring.**
Materials and methods: **Light from a Nd: YAG laser was utilized for thermotherapy. A theoretical model for calculating tissue temperature was used to predict the experimental results and to simulate in vivo treatments.**
Results: **The metal-covered tip produced carbonization and tissue vaporization that was not found with the diffuser. After 20 min of irradiation at a laser power of 7 W, the coagulated volumes with and without carbonization were found to be 13.1 cm^3 (range 12.4–14.1 cm^3, n = 4) and 12.2 cm^3 (range 11.5–13.4 cm^3, n = 4), respectively. Mathematical simulations showed that in unperfused tissue, a diffusing laser heat source produces smaller lesions than does a conductive heat source at the same power, the difference in coagulated volume becoming smaller with increased treatment time and increased power.**
Conclusion: **Using cylindrical diffusers, interstitial laser-induced thermotherapy without carbonization at the fiber tip can be as efficient as treatment with carbonization. Lasers Surg. Med. 22:51–57, 1998.** **© 1998 Wiley-Liss, Inc.**

Key words: charring; cylindrical diffuser; mathematical modeling; Nd:YAG laser

INTRODUCTION

Interstitial laser-induced thermotherapy (ILT) is a method of destroying deeply situated tumors by heating [1,2]. Laser light is transmitted in thin optical fibers, the tips of which are placed in the neoplasm. The most widely used laser for ILT has been the Nd:YAG laser, emitting near-infrared light at 1,064 nm. Tissue light penetration reaches a maximum in this wavelength region [3]. Different fiber tips have been employed for ILT. The earliest approaches relied on plane-cut fibers. Due to the small light-emitting area of these fibers, carbonization occurs at low power levels. Charred tissue absorbs light strongly, which converts the distributed light source to a near-point heat source [4]. It has been shown that at the same power and total energy, a near-point heat source produces a larger lesion than is obtained with deeply penetrating laser light emitted from a plane-cut fiber [5,6]. This has raised the question whether the laser should be used at all for interstitial thermotherapy. It is still obscure if carbonization is biologically disadvantageous. Theoretically, the cavity formation associated with charring could predispose to infection. Also, vaporization of tissue has been shown to give rise to intracardiac gas of unknown clinical significance [7].

With recent development in fiber applicators, such as cylindrical diffusers emitting light over an extended length, it has become possible to

*Correspondence to: Christian Sturesson, Department of Physics, Lund Institute of Technology, P.O. Box 118, S-221 00 Lund, Sweden. E-mail: christian.sturesson@fysik.lth.se

Accepted 10 October 1997

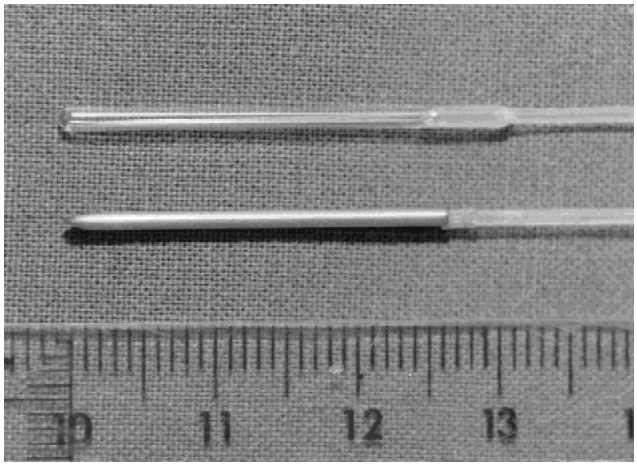

Fig. 1. Photograph of the developed cylindrical diffuser and the conductive near-line source made by covering the diffuser with a hollow steel needle.

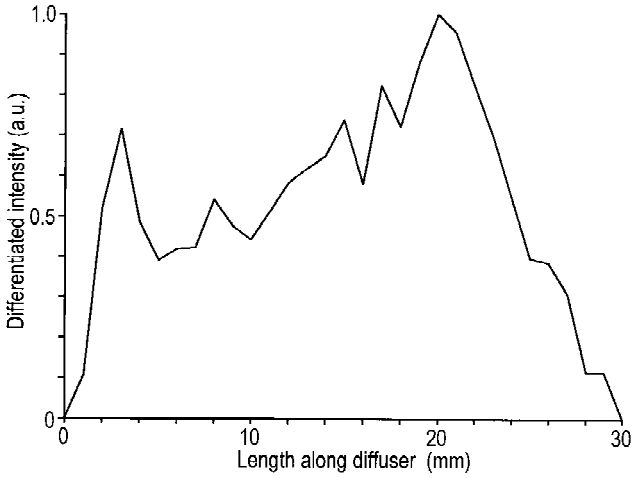

Fig. 2. Differentiated emitted intensity of the diffuser, measured by inserting the diffuser into an integrating sphere in steps of 1 mm.

produce coagulated lesions of clinically useful size without central charring [8]. However, if even larger lesions can be created by initiating the charring process around these diffusers, the choice of using the laser for thermotherapy still would be dubious.

The present study was performed to investigate the coagulated lesions produced using a cylindrical diffuser and a conductive near-line source. Experiments were performed in porcine muscle in vitro. A mathematical model was used to confirm the experimental results and to simulate in vivo treatments.

MATERIALS AND METHODS

A cylindrical diffuser was made by immersing the distal 25 mm of a fiber glass core into hydrofluoric acid stepwise, producing a tapered end [9]. The tip was then mechanically ground using a fine sandpaper, which gave the tip a frosted appearance. The fragile fiber end was protected by an 1.7 mm outer diameter glass dome. The dome was fixed onto the plastic fiber coating using a heat-resistant two component glue. Figure 1 shows a photograph of the developed diffuser. The emission profile of the diffuser was measured by inserting the tip in steps of 1 mm into an integrating sphere. For this measurement, chopped light from a He:Ne laser emitting at 633 nm was focused into the fiber. The power on the inside wall of the integrating sphere was measured with a photodiode and a lock-in amplifier. The average of three measurements of the emission profile was used to calculate the differentiated intensity of the diffusing fiber tip, which is shown in Figure 2.

A conductive near-line source was realized by covering the tapered tip of the optical fiber with a 25 mm ordinary medical steel needle, as shown in Figure 1. The tip of the needle was pinched, closing the distal end. The outer diameter of the needle was 1.2 mm. A metal-coated fiber tip can be regarded as a laser fiber tip irradiating optically opaque tissue, which can be an approximation for charred tissue [4].

ILT was performed in porcine muscle in vitro. Tissue was cut into $10 \times 10 \times 4$ cm^3 blocks. The tissue samples, closely wrapped in plastic foil to prevent water evaporation, were stored in the laboratory overnight at a temperature of 20 ± 1°C. After removing the foil, an applicator, prepared in either of the two ways presented above, was placed on top of a tissue sample in the center of the largest rectangular surface. Another tissue block was then put on top of the applicator. Laser light from a continuous wave Nd:YAG laser (Mod. 416, Quantronix Corp., Smithtown, NY), emitting at 1,064 nm, was focused into the fiber and ILT was performed for 5, 10, and 20 min at a power of 5 W and 7 W. Occasionally, temperature measurements were made using thermistors placed at a distance 10 mm and 15 mm radially out from the middle of the applicator. At least two experiments were made for each combination of laser power and treatment time. The power emitted at the distal end of the fiber was measured using an integrating sphere power meter (Mod. 2015, Laser

Therapeutics, Buellton, CA). Power measurement of the tip with the steel needle was performed before the needle was threaded onto the fiber tip. Back-reflection of light into the fiber was assumed negligible. Approximately 3 min after the irradiation was terminated, the two tissue blocks were separated and the longitudinal and transverse diameter of the visible whitish elliptical coagulated lesion were measured. The coagulated volume was calculated as $\pi d_1 d_2^2/6$, where d_1 (m) is the longitudinal length and d_2 (m) is the transverse length, as measured perpendicularly to and at the middle of the applicator. Additional experiments to measure the interstitial temperature distribution were made using an infrared camera (Agema Thermovision™ 860, Agema, Sweden). Within 1 sec after separating the two tissue blocks, the two-dimensional temperature distribution in the plane of the laser fiber was measured.

A mathematical model was used to numerically calculate the temperature rise in the heated tissue [10]. Monte Carlo simulations, using a modified version of a public domain computer program, were performed to calculate the light absorption distribution [11]. The optical properties of tissue, i.e., the absorption coefficient, μ_a (m^{-1}), scattering coefficient, μ_s (m^{-1}), and anisotropy factor, g (dimensionless), assuming a Henyey-Greenstein distribution of the scattered photons, were used as input parameters. The light absorption distribution then constituted source terms in the bio-heat equation:

$$\rho c \frac{\partial T}{\partial t} = \nabla(\lambda \nabla T) + Q_s + Q_p \qquad (1)$$

where T is the tissue temperature (K), ρ is the tissue density (kg m^{-3}), c is the specific heat of the tissue (J kg^{-1} K^{-1}), and λ is the thermal conductivity of the tissue (W m^{-1} K^{-1}). The time is represented by t (seconds), Q_s is the external laser heat-source term (W m^{-3}), and Q_p is the heat removal due to perfusion (W m^{-3}), which was modeled as a heat sink [12,13].

A finite difference model calculated the temperature rise in cylindrical coordinates using a grid size of $\Delta r = \Delta z = 0.5$ mm. The applicator was modeled as a transparent tube with a diameter of 2.0 mm. A perfectly diffusing line source was assumed in the distal 25 mm of the tube. When modeling the steel needle applicator, the absorption coefficient in the Monte Carlo simulations was set to 10^{30} cm^{-1}. This caused all energy to be deposited in the layer closest to the tube. The tip of the fiber was placed 65 mm below the top of the calculation domain, which constituted a cylinder with a 50 mm radius and a height of 120 mm. All boundaries were assumed insulated.

TABLE 1. Optical Properties Used in Monte Carlo Simulations[a]

Tissue	μ_a (cm^{-1})	μ_s (cm^{-1})	g
Turkey muscle	0.4	80	0.98
Porcine liver	0.5	80	0.97
Bovine muscle	1.2	13.3	0.79

[a]Adapted from Ref. 14.

Comparison between experimental and theoretical results of coagulated volumes was difficult due to the lack of the optical properties of porcine muscle in the literature. To investigate the influence of the optical properties on coagulated volume tissues with different optical penetration depths were considered. The parameters used in the Monte Carlo simulations, which have been measured at 1,064 nm, are shown in Table 1 [14]. The tissues included in the parametric study were bovine muscle, procine liver, and turkey muscle. Experimental results from ILT in vitro have shown that the optical penetration depth of porcine muscle most likely is in between that of bovine muscle and chicken muscle [4,5].

The properties characterizing the thermal behavior of tissue were calculated by assuming a tissue mass water fraction of 70% [15,16]. Vaporization effects were not included in the model. The tissue damage caused by the temperature rise following laser irradiation was represented by a damage integral based on an Arrhenius relationship [17].

$$\Omega(r,z) = A \int \exp \frac{-\Delta E}{R \times T(r,z,t)}\, dt \qquad (2)$$

where Ω represents the degree of coagulation (dimensionless), A is the frequency factor (s^{-1}), ΔE is the activation energy (J $mole^{-1}$), R is the universal gas constant equal to 8.314 J $mole^{-1}$ K^{-1}, and T is the tissue temperature (K). The values of A and ΔE were taken to be $A = 3.1 \times 10^{98}$ s^{-1} and $\Delta E = 6.27 \times 10^5$ J $mole^{-1}$ [17]. A value of the damage integral >1.0 was assumed to produce visible coagulation. The model was used to simulate the in vitro experiments. The initial tissue temperature was then set to 20°C.

In vivo treatment was simulated to investigate the influence of blood perfusion and of in-

creasing the initial tissue temperature to body core temperature (37°C). For each simulated treatment with the diffuser, the laser power was chosen to result in a maximum tissue temperature equal to 100°C after 20 min of heating, which was assumed to prevent carbonization. Depending on blood perfusion and tissue type, different power levels were obtained. Two simulations at each power level were performed: with the diffuser (no carbonization) and with the metal-covered tip (carbonization). The blood perfusion rate used in Equation 1 was taken to be either zero or 30 ml min^{-1} 100 g^{-1}, which is a value representative of various human tumors [18].

RESULTS

The diffusing tip created ellipsoidal coagulated lesions without central charring in all experiments. The metal-covered tip also produced ellipsoidal coagulated lesions, but with pronounced carbonization around the tip. Using the steel-covered tip, hot vapor was frequently found to dissect between the two tissue samples, creating a narrow bulbous coagulation zone, a few mm thick, radiating out from the tip. When the vapor-produced coagulation interfered with measurements of longitudinal or transverse coagulation lengths, the coagulated lesion was considered to be symmetric with respect to the transverse and longitudinal axis of the applicator, respectively. The measurement uncertainty was typically ± 1 mm between the experiments performed at each power setting and irradiation time. Tissue temperature measurements revealed a linear increase in temperature at both 10 mm and 15 mm from the applicator during the 20-min treatment sessions (results not shown).

Figure 3 shows the measured and calculated volumes of coagulation. The shaded area is bounded by the curves obtained by incorporating the optical properties of bovine muscle (upper boundary) and turkey muscle (lower boundary) into the calculations. Light penetrates bovine muscle less than it does turkey muscle. The broken line represents the calculated results using the optical properties of porcine liver. Figure 4 shows the measured and calculated temperature distributions after 770 sec of irradiation at 5 W with the diffuser, using the optical properties of porcine liver in the simulations.

The theoretical results after incorporating blood perfusion in the model and increasing the initial tissue temperature to 37°C are shown in

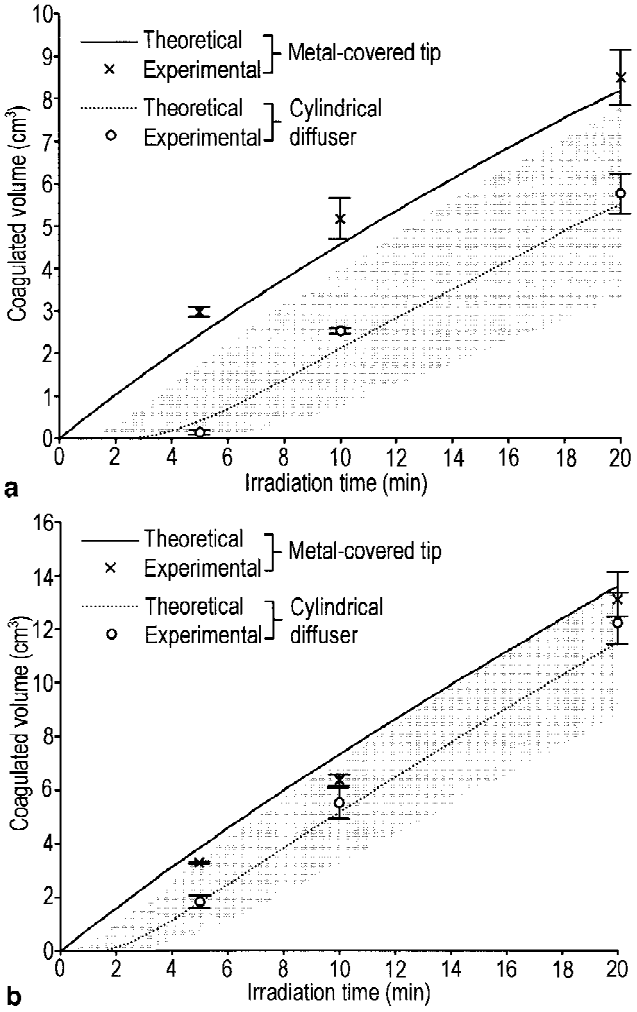

Fig. 3. **(a)** Measured and calculated coagulated volumes after treatment with the diffuser and the metal-covered tip at a laser power of 5 W. Error bars indicate the range of measured values. The broken line was calculated for porcine liver. The shaded area is bounded by the calculated results for bovine muscle (upper boundary) and turkey muscle (lower boundary). **(b)** As Figure 3(a) but as a laser power of 7 W.

Figure 5. Figure 5a depicts the ratio between the coagulated volumes obtained without and with carbonization as a function of treatment time. Figure 5b shows the coagulated volumes after 20 min of irradiation using different optical properties.

DISCUSSION

Plane-cut fibers have frequently been employed in ILT. Both experimental and theoretical evidence exist stating that carbonization at the bare fiber-tip in ILT creates larger lesions due to the light absorptive properties of carbonized tis-

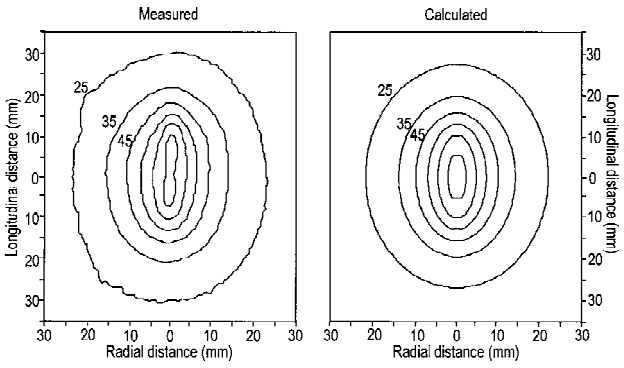

Fig. 4. Measured and calculated two-dimensional temperature distributions in the plane of the cylindrical diffuser evaluated after 770 s at a laser power of 5 W. Calculation results were obtained using the optical properties of porcine liver as input parameters. The contours are at 10°C interval starting at 25°C.

sue [5,6,19–21]. Therefore, some investigators have deliberately induced charring around the tip before treatment. The clinical importance of charring during ILT is still not fully elucidated. If carbonization proves harmless or even advantageous to the treatment result, expensive lasers could easily be outdone by cheap resistive heating elements [22]. The only obvious reasons to use lasers would then be the nonmetallic energy delivery provided by the optical fibers, permitting noninvasive temperature measurements with the technique of magnetic resonance imaging [23], and the possibility to combine heat treatment with photodynamic therapy [24].

With the advent of heat-resistant cylindrical diffusers, clinically significant tissue volumes can be coagulated without central charring. By employing multiple fibers larger tumors can be thermally eradicated [25,26]. Charring at the diffuser surface would then intuitively lead to even greater lesions. The present study was performed to investigate the influence of carbonization on coagulated volume using cylindrical diffusers.

Experiments in vitro showed that the steel-covered tip produced larger lesions than did the diffuser. The metal-coated tip acts much like a precharred tip. The difference in coagulated volume became smaller when using greater laser powers and when irradiating for longer times. Central charring was always present with the metal-covered tip, whereas no carbonization was produced with the diffuser using the present power settings. With the diffuser, the maximum transverse coagulation length was found to be 27 mm. Ellipsoidal-shape volumes of up to 13 cm^3

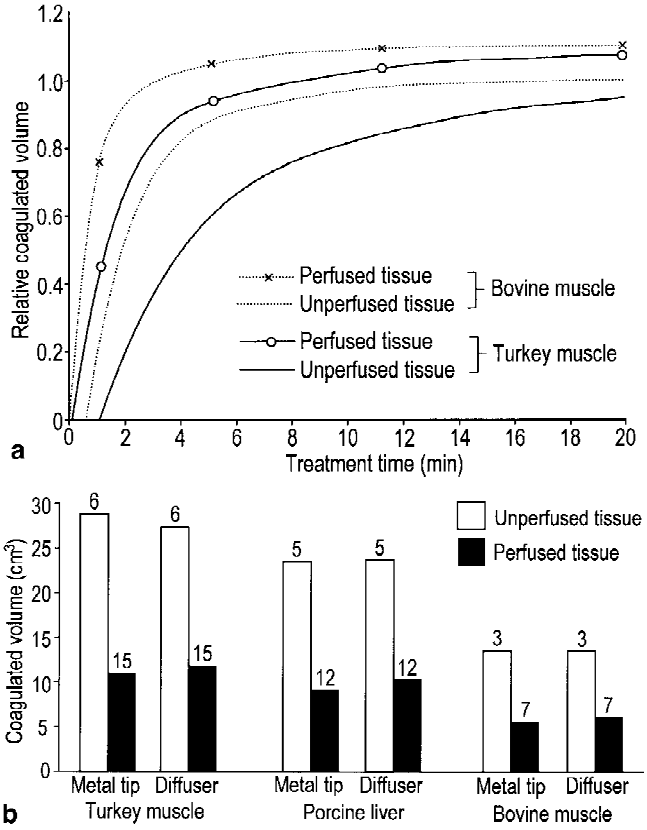

Fig. 5. **(a)** Calculated relative coagulated volumes (that is, ratio between coagulated volumes with and without carbonization) after treatment of tissue at an initial temperature of 37°C in perfused and unperfused tissue. **(b)** Calculated coagulated volumes after 20 min of irradiation with and without carbonization and blood perfusion for tissues with different optical properties. Values above each bar indicate the laser power used in the simulations. With stated values of the laser power the maximum tissue temperature was 100°C after treatment for 20 min with the diffuser.

were in this way coagulated without charring. The coagulated volume was found to increase linearly with time, corresponding to a linear increase in tissue temperature (results not shown).

The advantageous effect of charring in creating greater lesions is minimized when using high powers, as shown in Figure 3. Carbonization is initiated after the tissue is dehydrated [27]. If carbonization is to be prevented, extreme dehydration should be avoided. This is probably accomplished by maintaining the maximum tissue temperature below the boiling point of water, which limits the maximum laser power that can be employed. Because different tissues have different optical properties, it is difficult to conclude beforehand the maximum laser power. Temperature measurements close to the fiber tip would then be necessary.

The theoretical calculations employing the optical properties of porcine liver accurately predicted the measured coagulated volumes in porcine muscle. Also, the measured and calculated temperature distributions showed considerable similarity (Fig. 4), which indicates that the used optical properties and the constants employed in the Arrhenius relationship (Equation 2) are valid. Although vaporization was not included in the model, good agreement between theory and experiment was found when modeling the steel-covered tip.

The theoretical model was then used to investigate the effect of increasing the initial tissue temperature to body-core temperature and incorporating blood perfusion, under the restriction that the maximum tissue temperature when modeling the diffuser should be equal to 100°C. Blood perfusion plays a significant role in limiting the thermal damage resulting after ILT [28]. Theoretically, it was found that in perfused tissues treatment with charring resulted in slightly smaller coagulated volumes as compared with treatment without charring after 20 minutes. Simulated treatment in unperfused tissue resulted in approximately equal treatment volumes after 20 min whether charring was present or not. In this case, the treated volume increased rapidly even after 20 min (results not shown). By comparing the treatment volumes obtained with and without perfusion, it was found that charring is predicted to influence the treatment result only to a minor extent (Fig. 5b). In attempts to maximize the necrotic volume during ILT, the main issue should then be to minimize blood perfusion. However, it is indicated that charring is advantageous during short treatments especially in lightly pigmented tissues (Fig. 5a).

In conclusion, the present study has showed that, at the same power in unperfused tissue, carbonization at a cylindrical diffusing fiber tip creates a greater lesion as compared with when charring is avoided. The difference in coagulated volume becomes smaller with increased treatment time making the two methods with and without charring approximately equally efficient. In perfused tissue, calculations showed that after 20 min of treatment the coagulated volumes without charring were somewhat greater than the volumes obtained with carbonization. Thus, with proper treatment parameters, little or nothing is expected to be gained by inducing carbonization around the cylindrical diffuser with respect to lesion size. If avoiding carbonization proves to be biologically advantageous in interstitial thermotherapy, the presented results point to that the laser could be a suitable choice for inducing thermal tumor destruction.

ACKNOWLEDGMENTS

The support of Dr. S Andersson-Engels and Prof. S Svanberg, Department of Physics, Lund Institute of Technology, is gratefully acknowledged. The author is very grateful to Prof B R Persson, Department of Radiation Physics, Lund University Hospital, for providing the thermocamera. This work was financially supported by the Swedish Natural Science Research Council and the Swedish Research Council of Engineering Sciences.

REFERENCES

1. Steger AC, Lees WR, Walmsley K, Bown SG. Interstitial laser hyperthermia: A new approach to local destruction of tumours. Br Med J 1989; 299:362–365.
2. Dowlatshahi K, Bhattacharya AK, Silver B, Matalon T, Williams JW. Percutaneous interstitial laser therapy of a patient with recurrent hepatoma in a transplanted liver. Surgery 1992; 112:603–606.
3. Parsa P, Jacques SL, Nishioka NS. Optical properties of rat liver between 350 and 2200 nm. Appl Opt 1989; 28: 2325–2330.
4. Wyman D, Wilson B, Adams K. Dependence of laser photocoagulation on interstitial delivery parameters. Lasers Surg Med 1994; 14:59–64.
5. Wyman DR, Whelan WM, Wilson BC. Interstitial laser photocoagulation: Nd:YAG 1064 nm optical fiber compared to point heat source. Lasers Surg Med 1992; 12: 659–664.
6. Wyman DR. Whelan WM. Basic optothermal diffusion theory for interstitial laser photocoagulation. Med Phys 1994; 21:1651–1656.
7. Malone DE, Lesiuk L, Brady AP, Wyman DR, Wilson BC. Hepatic interstitial laser photocoagulation: Demonstration and possible clinical importance of intravascular gas. Radiology 1994; 193:233–237.
8. van Hillegersberg R, van Staveren HJ, Kort WJ, Zondervan PE, Terpstra OT. Interstitial Nd:YAG laser coagulation with a cylindrical diffusing fiber tip in experimental liver metastases. Lasers Surg Med 1994; 14:124–138.
9. Sturesson C, Andersson-Engels S. Tissue temperature control using a water-cooled applicator: Implications for transurethral laser-induced thermo-therapy of benign prostatic hyperplasia. Med Phys 1997; 24:461–470.
10. Sturesson C, Andersson-Engels S. A mathematical model for predicting the temperature distribution in laser-induced hyperthermia: Experimental evaluation and applications. Phys Med Biol 1995; 40:2037–2052.
11. Wang L, Jacques SL, Zheng L. MCML—Monte Carlo modelling of light transport in multi-layered tissues. Comp Meth Prog Biomed 1995; 47:131–146.
12. Pennes HH. Analysis of tissue and arterial blood tem-

peratures in the resting human forearm. J Appl Physiol 1948; 1:93–122.
13. Moros Eg, Dutton AW, Roemer RB, Burton M, Hynynen. Experimental evaluation of two simple thermal models using hyperthermia in muscle in vivo. Int J Hyperthermia 1993; 9:581–598.
14. Roggan A, Dörschel K, Minet O, Wolff D, Müller G. The optical properties of biological tissue in the near infrared wavelength range—review and measurements. In: Müller G, Roggan A, eds. "Laser-induced Interstitial Thermotherapy." Bellingham, WA: SPIE, 1995, pp 10–44.
15. Welch AJ. The thermal response of laser irradiated tissue. IEEE J Quant Electr 1984; 20:1471–1481.
16. Jacques SL, Prahl SA. Modeling optical and thermal distribution in tissue during laser irradiation. Lasers Surg Med 1987; 6:494–503.
17. Henriques FC, Studies of thermal injury. Arch Pathol 1947; 43:489–502.
18. Jain RK, Ward-Hartley K. Tumor blood flow—characterization, modifications, and role in hyperthermia. IEEE Trans Sonics Ultrasonics 1984; 31:504–526.
19. Amin Z, Buonaccorsi G, Mills T, Harries S, Lees WR, Bown SG. Interstitial laser photocoagulation: Evaluation of a 1320 nm Nd:YAG and an 805 nm diode laser: The significance of charring and the value of precharring the fibre tip. Lasers Med Sci 1993; 8:113–120.
20. Harries SA, Amin Z, Smith EF, Lees WR, Cooke J, Cook MG, Scurr JH, Kissin MW, Bown SG. Interstitial laser photocoagulation as a treatment for breast cancer. Br J Surg 1994; 81:1617–1619.
21. Jacques SL. Role of tissue optics and pulse duration on tissue effects during high-power laser irrdiation. Appl Opt 1993; 32:2447–2454.
22. Haider SA, Cetas TC, Roemer RB. Temperature distribution in tissues from a regular array of hot source implants: an analytical approximation. IEEE Trans Biomed Eng 1993; 40:408–417.
23. Jolesz FA, Bleier AR, Jakab P, Ruenzel PW, Huttl K, Jako GJ. MR imaging of laser-tissue interactions. Radiology 1988; 168:249–253.
24. Liu DL, Andersson-Engels S, Sturesson C, Svanberg K, Håkansson CH, Svanberg S. Tumour vessel damage resulting from laser-induced hyperthermia alone and in combination with photodynamic therapy. Cancer Lett 1997; 111:157–165.
25. Steger AC, Lees WR, Shorvon P, Walmsley K, Bown SG. Multiple-fibre low-power interstitial laser hyperthermia: Studies in the normal liver. Br J Surg 1992; 79:139–145.
26. Ivarsson K, Olsrud J, Sturesson C, Möller PH, Persson BR, Tranberg KG. A feedback interstitial diode laser (805 nm) thermotherapy system: ex vivo evaluation and mathematical modeling with one and four fibers. Lasers Surg Med (in press).
27. LeCarpentier GL, Motamedi M, McMath LP, Rastegar S, Welch AJ. Continuous wave laser ablation of tissue: Analysis of thermal and mechanical events. IEEE Trans Biomed Eng 1993; 40:188–200.
28. Sturesson C, Liu DL, Stenram U, Andersson-Engels S. Hepatic inflow occlusion increases the efficacy of interstitial laser-induced thermotherapy in rat. J Surg Res 1997; 71:67–72.